ISSN 1007-9327 (print)
ISSN 2219-2840 (online)

World Journal of *Gastroenterology*

World J Gastroenterol 2019 April 28; 25(16): 1907-2018

Published by Baishideng Publishing Group Inc

World Journal of Gastroenterology

Contents

Weekly Volume 25 Number 16 April 28, 2019

CASE REPORT

ABOUT COVER

Editorial board member of *World Journal of Gastroenterology*, Gwang Ha Ha Kim, MD, PhD, Full Professor, Department of Internal Medicine, Pusan National University School of Medicine, Busan 49241, South Korea

AIMS AND SCOPE

World Journal of Gastroenterology (*World J Gastroenterol*, *WJG*, print ISSN 1007-9327, online ISSN 2219-2840, DOI: 10.3748) is a peer-reviewed open access journal. The *WJG* Editorial Board consists of 642 experts in gastroenterology and hepatology from 59 countries.

The primary task of *WJG* is to rapidly publish high-quality original articles, reviews, and commentaries in the fields of gastroenterology, hepatology, gastrointestinal endoscopy, gastrointestinal surgery, hepatobiliary surgery, gastrointestinal oncology, gastrointestinal radiation oncology, *etc*. The *WJG* is dedicated to become an influential and prestigious journal in gastroenterology and hepatology, to promote the development of above disciplines, and to improve the diagnostic and therapeutic skill and expertise of clinicians.

INDEXING/ABSTRACTING

The *WJG* is now indexed in Current Contents®/Clinical Medicine, Science Citation Index Expanded (also known as SciSearch®), Journal Citation Reports®, Index Medicus, MEDLINE, PubMed, PubMed Central, Scopus and Directory of Open Access Journals. The 2018 edition of Journal Citation Report® cites the 2017 impact factor for *WJG* as 3.300 (5-year impact factor: 3.387), ranking *WJG* as 35th among 80 journals in gastroenterology and hepatology (quartile in category Q2).

RESPONSIBLE EDITORS FOR THIS ISSUE

Responsible Electronic Editor: *Han Song* **Proofing Editorial Office Director:** *Ze-Mao Gong*

NAME OF JOURNAL
World Journal of Gastroenterology

ISSN
ISSN 1007-9327 (print) ISSN 2219-2840 (online)

LAUNCH DATE
October 1, 1995

FREQUENCY
Weekly

EDITORS-IN-CHIEF
Subrata Ghosh, Andrzej S Tarnawski

EDITORIAL BOARD MEMBERS
http://www.wjgnet.com/1007-9327/editorialboard.htm

EDITORIAL OFFICE
Ze-Mao Gong, Director

PUBLICATION DATE
April 28, 2019

INSTRUCTIONS TO AUTHORS
https://www.wjgnet.com/bpg/gerinfo/204

GUIDELINES FOR ETHICS DOCUMENTS
https://www.wjgnet.com/bpg/GerInfo/287

GUIDELINES FOR NON-NATIVE SPEAKERS OF ENGLISH
https://www.wjgnet.com/bpg/gerinfo/240

PUBLICATION MISCONDUCT
https://www.wjgnet.com/bpg/gerinfo/208

ARTICLE PROCESSING CHARGE
https://www.wjgnet.com/bpg/gerinfo/242

STEPS FOR SUBMITTING MANUSCRIPTS
https://www.wjgnet.com/bpg/GerInfo/239

ONLINE SUBMISSION
https://www.f6publishing.com

World Journal of Gastroenterology

Submit a Manuscript: https://www.f6publishing.com

World J Gastroenterol 2019 April 28; 25(16): 1997-2009

DOI: 10.3748/wjg.v25.i16.1997

ISSN 1007-9327 (print) ISSN 2219-2840 (online)

ORIGINAL ARTICLE

Observational Study

Assessment of chronic radiation proctopathy and radiofrequency ablation treatment follow-up with optical coherence tomography angiography: A pilot study

Osman Oguz Ahsen, Kaicheng Liang, Hsiang-Chieh Lee, Zhao Wang, James G Fujimoto, Hiroshi Mashimo

ORCID number: Osman Oguz Ahsen (0000-0003-4811-3429); Kaicheng Liang (0000-0003-3237-4034); Hsiang-Chieh Lee (0000-0002-2976-6195); Zhao Wang (0000-0002-3628-5699); James G Fujimoto (0000-0002-0828-4357); Hiroshi Mashimo (0000-0002-6132-6771).

Author contributions: Fujimoto JG, Mashimo H, Ahsen OO designed the study; Ahsen OO, Liang K, Lee HC developed the OCT imaging technology; Ahsen OO, Liang K, Lee HC, Wang Z collected the data; Ahsen OO and Liang K analyzed the OCT and OCTA data; Fujimoto JG and Mashimo H obtained funding for the study; Ahsen OO, Fujimoto JG and Mashimo H wrote the manuscript; all authors read the manuscript; Fujimoto JG and Mashimo H are principal investigators for this study.

Supported by facility supports of the VA Boston Healthcare System, NIH grants R01-CA075289-21 (JGF and HM), Air Force Office of Scientific Research contract FA9550-15-1-0473 (JGF).

Institutional review board statement: This study was conducted under protocols at the Veteran Affairs Boston Healthcare System (VABHS) Institutional Review Board (IRB), Harvard Medical School (HMS) Office of Human Research Administration (OHRA) and Massachusetts Institute of Technology (MIT) Committee on the Use of Humans as Experimental Subjects

Osman Oguz Ahsen, Kaicheng Liang, Hsiang-Chieh Lee, Zhao Wang, James G Fujimoto, Department of Electrical Engineering and Computer Science, Massachusetts Institute of Technology, Cambridge, MA 02139, United States

Hiroshi Mashimo, Gastroenterology Section, VA Boston Healthcare System, Harvard School of Medicine, Boston, MA 02130, United States

Corresponding author: Hiroshi Mashimo, MD, MSc, PhD, Associate Professor, Research Scientist, Gastroenterology Section, VA Boston Healthcare System, Harvard School of Medicine, 150 South Huntington Ave., Boston, MA 02130, United States.
hmashimo@hms.harvard.edu
Telephone: +1-857-2035640
Fax: +1-857-2035666

Abstract

BACKGROUND

Chronic radiation proctopathy (CRP) occurs as a result of pelvic radiation therapy and is associated with formation of abnormal vasculature that may lead to persistent rectal bleeding. While incidence is declining due to refinement of radiation delivery techniques, CRP remains one of the major complications of pelvic radiation therapy and significantly affects patient quality of life. Radiofrequency ablation (RFA) is an emerging treatment modality for eradicating abnormal vasculature associated with CRP. However, questions remain regarding CRP pathophysiology and optimal disease management.

AIM

To study feasibility of optical coherence tomography angiography (OCTA) for investigating subsurface vascular alterations in CRP and response to RFA treatment.

METHODS

Two patients with normal rectum and 8 patients referred for, or undergoing endoscopic RFA treatment for CRP were imaged with a prototype ultrahigh-speed optical coherence tomography (OCT) system over 15 OCT/colonoscopy visits (2 normal patients, 5 RFA-naïve patients, 8 RFA-follow-up visits). OCT and OCTA was performed by placing the OCT catheter onto the dentate line and rectum without endoscopic guidance. OCTA enabled depth-resolved microvasculature imaging using motion contrast from flowing blood, without

(COUHES).

Informed consent statement: All study participants provided informed written consent prior to study enrollment.

Conflict-of-interest statement: We have no relevant financial relationships to disclose.

Data sharing statement: No additional data are available.

STROBE statement: Guidelines of the STROBE Statement have been adopted.

Manuscript source: Unsolicited manuscript

Received: November 10, 2018
Peer-review started: November 12, 2018
First decision: December 28, 2018
Revised: February 12, 2019
Accepted: February 15, 2019
Article in press: February 16, 2019
Published online: April 28, 2019

P-Reviewer: Kamimura K, Kharlamov AN, Kupeli S
S-Editor: Yan JP
L-Editor: A
E-Editor: Song H

requiring injected dyes. OCTA features of normal and abnormal microvasculature were assessed in the mucosa and submucosa. Blinded reading of OCTA images was performed to assess the association of abnormal rectal microvasculature with CRP and RFA treatment, and rectal telangiectasia density endoscopic scoring.

RESULTS

OCTA/OCT images are intrinsically co-registered and enabled depth-resolved visualization of microvasculature in the mucosa and submucosa. OCTA visualized normal vascular patterns with regular honeycomb patterns *vs* abnormal vasculature with distorted honeycomb patterns and ectatic/tortuous microvasculature in the rectal mucosa. Normal arterioles and venules < 200 μm in diameter versus abnormal heterogenous enlarged arterioles and venules > 200 μm in diameter were visualized in the rectal submucosa. Abnormal mucosal vasculature occurred in 0 of 2 normal patients and 3 of 5 RFA-naïve patients, while abnormal submucosal vasculature occurred more often, in 1 of 2 normal patients and 5 of 5 RFA-naïve patients. After RFA treatment, vascular abnormalities decreased, with abnormal mucosal vasculature observed in 0 of 8 RFA-follow-up visits and abnormal submucosal vasculature observed in only and 2 of 8 RFA-follow-up visits.

CONCLUSION

OCTA visualizes depth-resolved microvascular abnormalities in CRP, allowing assessment of superficial features which are endoscopically visible as well as deeper vasculature which cannot be seen endoscopically. OCTA/OCT of the rectum can be performed in conjunction with, or independently from endoscopy. Further studies are warranted to investigate if OCTA/OCT can elucidate pathophysiology of CRP or improve management.

Key words: Optical coherence tomography; Optical coherence tomography angiography; Radiofrequency ablation; Chronic radiation proctopathy; Rectal telangiectasia density scoring system; Subsurface microvascular imaging

Core tip: In this study we use a prototype ultrahigh-speed optical coherence tomography (OCT) system and OCT angiography (OCTA) to perform depth-resolved visualization of microvasculature in the mucosal and submucosal layers of the rectum without requiring injected dyes. Abnormal distorted honeycomb patterns and ectatic/tortuous microvasculature in the rectal mucosa and heterogenous enlarged arterioles and venules > 200 μm in diameter in the submucosa are associated with chronic radiation proctopathy and resolved with radiofrequency ablation treatment. OCTA/OCT is a promising tool for investigating the pathophysiology of chronic radiation proctopathy and further studies are warranted to understand if it can help in clinical management.

Citation: Ahsen OO, Liang K, Lee HC, Wang Z, Fujimoto JG, Mashimo H. Assessment of chronic radiation proctopathy and radiofrequency ablation treatment follow-up with optical coherence tomography angiography: A pilot study. *World J Gastroenterol* 2019; 25(16): 1997-2009
URL: https://www.wjgnet.com/1007-9327/full/v25/i16/1997.htm
DOI: https://dx.doi.org/10.3748/wjg.v25.i16.1997

INTRODUCTION

Chronic radiation proctopathy (CRP) occurs as a result of pelvic radiation therapy and is associated with formation of abnormal vascular lesions that may lead to persistent rectal bleeding. Up to 20% of patients receiving radiation therapy for prostate and cervical cancer may develop CRP[1]. While the incidence is declining[2,3] due to refinement of radiation delivery techniques[4-6], CRP remains one of the major complications of pelvic radiation therapy and significantly affects patient quality of

life. For symptomatic patients with prior pelvic radiation therapy, the current clinical standard for diagnosis and assessment of disease severity for CRP is colonoscopy or sigmoidoscopy[7]; which examine rectal mucosa for CRP hallmarks, such as hemorrhage, ulcerations and telangiectasias[8]. The rectal telangiectasia density (RTD) scoring system was developed for endoscopic assessment of CRP and was shown to have a good correlation with clinical symptomatic assessment[9]. In this scoring system, endoscopic appearance is evaluated based on telangiectasia density and vascular coalescence, and a score from 0 to 3 is assigned. Biopsies can be taken during the endoscopy to rule out other diseases associated with abnormal vascular lesions (such as inflammatory bowel disease), but are recommended only for select cases due to the potential of further bleeding, ulcerations, and fistulae formation[10].

Management options for CRP range from non-endoscopic treatment with topical or oral medications, to endoscopic interventions such as dilation[11], bipolar electrocoagulation[12], argon plasma coagulation (APC)[13], cryotherapy[14], laser ablation[15] and radiofrequency ablation (RFA)[16]. More severe and refractory cases of CRP may necessitate surgical interventions such as colostomy and proctectomy[17,18]. Due to varying degrees of invasiveness and associated morbidity and mortality, it is essential to choose the optimal treatment strategy, which may begin by employing the least invasive non-endoscopic approaches such as observation or medical therapy, and escalate in accord with patient's response to the interventions[19].

Optical coherence tomography (OCT) enables three-dimensional visualization of tissue microstructure and was recently commercialized as volumetric laser endomicroscopy (NinePoint Medical, Bedford, MA, United States)[20,21]. Previous OCT studies have primarily focused on upper gastrointestinal pathologies such as Barrett's esophagus (BE), and have shown utility in endoscopic surveillance for detecting dysplastic lesions that are indiscernible under white light endoscopy[22,23]. We have recently developed an ultrahigh-speed OCT system which is more than 10 times faster than commercial instruments and can acquire volumetric images with higher transverse resolution and voxel density. The ultrahigh imaging speed also enables visualization of depth-resolved *en face* mucosal and microvascular features (known as OCT angiography, OCTA), in addition to cross-sectional and *en face* OCT imaging[24].

This pilot study investigated OCTA for assessing subsurface tissue microvasculature around the dentate line and rectum of normal patients as well as CRP patients who were RFA-naïve or had previous RFA treatments. OCT imaging was performed by directly placing the OCT catheter into the rectum of the patients without endoscopic guidance. OCTA enabled depth-resolved visualization of microvasculature, and OCTA features of normal and abnormal rectal microvasculature were described. Blinded reading of the OCTA features were performed to demonstrate association of abnormal rectal microvasculature with CRP and RFA treatment, and the RTD endoscopic scoring system.

MATERIALS AND METHODS

Study setting and patient requirement

This study was conducted at the Veteran Affairs Boston Healthcare System. Two patients with normal rectum and 8 patients referred for, or undergoing endoscopic treatment with RFA for CRP were enrolled in the study between October 2013 and November 2016 (n = 10). Five of the CRP patients were RFA-naïve at the baseline visit (time of initial OCT imaging), while 3 patients had previous RFA treatments. Five of the CRP patients imaged at the baseline visit were also imaged at RFA-follow-up visits within the study period, yielding a total of 15 OCT/colonoscopy visits 2 normal patients, 5 RFA-naïve patients, 8 RFA-follow-up visits). OCT imaging was performed during scheduled colonoscopy visits immediately before the colonoscopy procedure. Standard rectal examination with the colonoscope was conducted subsequent to OCT imaging. RFA was performed in patients with active rectal bleeding and/or based on endoscopic indication. A focal ablation catheter (Barrx 90, Medtronic, MN, United States) attached to the colonoscope (CF-HQ190L or CF-2T160, Olympus, Japan) typically in the six o'clock position and applied to the rectal mucosa with the endoscope retroflexed, as previously described[16]. Patient charts were reviewed to obtain information about rectal bleeding status and hemoglobin concentrations before and after the colonoscopy visits.

Ultrahigh-speed OCT system

OCT imaging was performed with a prototype ultrahigh-speed OCT system operating at an axial (depth) scan repetition rate of 600 kHz and a micromotor catheter imaging at 400 frames per second[24]. The depth and lateral image resolutions were 8 μm and 20

μm (full width at half maximum, in tissue), respectively, and the imaging range was 2.4 mm (in tissue). OCT datasets from the anterior side of the dentate line and rectum were acquired by directly placing the OCT catheter onto the dentate line and rectum of the patients without endoscopic guidance, but with real-time OCT imaging guidance. OCTA images were generated by calculating the intensity changes between sequential frames, and enabled depth-resolved imaging of microvasculature using motion contrast from flowing blood, without requiring injected dyes[24]. Each OCTA/OCT dataset covered an area of 10 mm × 16 mm (circumferential x longitudinal) and was acquired in 8 seconds. *En face* OCT and OCTA images at a given depth were viewed by summing over +/-50 μm depth (100 μm projection range) to improve contrast and reduce noise. Multiple acquisitions were performed by varying OCT catheter placement around the dentate line, guided by real-time OCT imaging, to ensure that the squamocolumnar junction and a distal margin of ± 2 cm were captured in the images.

Endoscopic grading of CRP severity and validation of OCTA assessment

Endoscopic RTD scores were assigned by the study physician (H.M.) during or shortly after the colonoscopy procedure, who was blinded to the OCTA assessment. All OCT and OCTA images were reviewed by a researcher experienced in OCT and OCTA interpretation (O.O.A.), who was not blinded to the clinical status of the patients. Rectal mucosal and submucosal microvasculature was assessed in normal and CRP patients, in conjunction with standard histology literature on rectal vasculature[25], to determine normal and abnormal microvascular features. All OCTA images were then read by another researcher experienced in OCT and OCTA interpretation (K.C.L.) to assess occurrence of abnormal microvascular features in the mucosal and submucosal layers. This reader assessed depth-resolved *en face* OCTA images in conjunction with the cross-sectional and *en face* OCT images in order to visualize the structure of and delineate between the mucosal and submucosal layers. This reader was blinded to the clinical status and RTD scores of the patients.

Normal and abnormal rectal OCTA features

Examples of OCT and OCTA images of rectal microstructural and microvascular architecture of normal and CRP patients are shown in Figures 1-3. Cross-sectional OCT images show mucosal and submucosal layers, while cross-sectional OCTA shows the location of vasculature relative to structural features. Vascular features exhibit a shadowing effect because structures located below large vessels fluctuate with blood flow. *En face* OCT and OCTA images summed over 100 μm projection range in the mucosa *vs* submucosa enable separate visualization of features at varying depths. Based on review of the images, OCTA features of normal and abnormal microvasculature were defined as follows (Figure 4): Normal rectal mucosal microvasculature consisted of a honeycomb-like microvascular pattern corresponding to subsurface capillary network described in the literature[25]. Abnormal rectal mucosal microvasculature had distortions to the honeycomb-like microvascular pattern, and had ectatic and tortuous microvasculature. Normal rectal submucosal microvasculature consisted of arterioles and venules with homogeneous vessel diameters typically of < 200 μm[25], in addition to shadowing from the superficial mucosal microvasculature. Abnormal rectal submucosal microvasculature consisted of arterioles and venules with heterogonous and unusually high vessel diameters (> 200 μm).

Statistical analysis

MATLAB (Mathworks, Inc, MA, United States) was used to perform all statistical calculations. Quantitative metrics were represented as mean ± standard deviation. A two-tailed t-test was used to compare the quantitative metrics between the continuous variables. A p-value of < 0.05 was considered statistically significant.

RESULTS

Patient demographics and baseline clinical status

Patient demographics are summarized in Table 1. Previously-treated patients had a mean of 2 RFA sessions prior to this study (range: 1-3). Baseline RTD scores were significantly different between the RFA-naïve and the previously-treated patients (mean score: 2 ± 0.7 *vs* 0.3 ± 0.6, respectively, $P = 0.007$). While the mean hemoglobin concentrations were higher for the previously-treated patients compared to RFA-naïve patients, the difference did not reach statistical significance (mean: 13.7 ± 1.8 g/dL *vs* 12 ± 0.8 g/dL, respectively, $P = 0.23$). 4 out of 5 (80%) RFA-naïve patients presented with rectal bleeding at the baseline visit, while none of the previously-

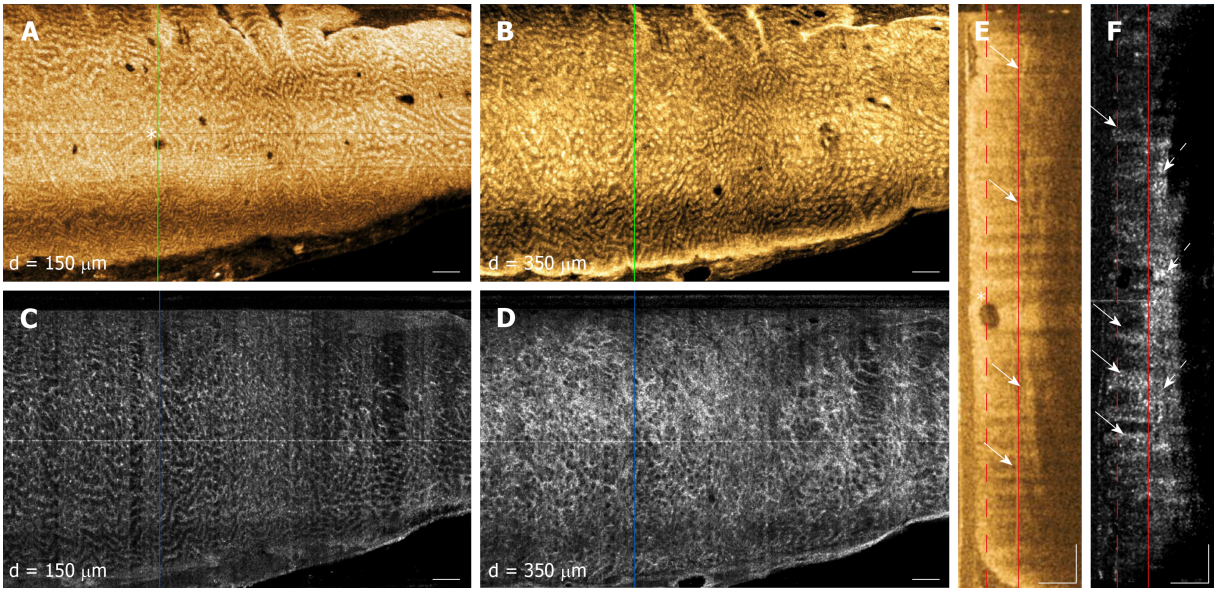

Figure 1 Depth-resolved *en face* optical coherence tomography and optical coherence tomography angiography images and cross-sectional optical coherence tomography and optical coherence tomography angiography images of a normal rectum. A: *En face* optical coherence tomography (OCT) image at 150 μm depth; B: *En face* OCT at 350 μm depth showing regular circular mucosal patterns characteristics of normal rectum; C: *En face* OCT angiography (OCTA) image at 150 μm depth showing regular honeycomb-like microvascular pattern of the subsurface capillary network in the mucosal layer; D: *En face* OCTA image at 350 μm depth showing rectal microvasculature corresponding to arterioles and venules in the submucosal layer, in addition to shadowing from the superficial mucosal microvasculature; E: Cross-sectional OCT image from the solid green lines in A and B, showing regular columnar architecture of normal rectum. The submucosal layer can be identified by the vertical layers traversing across the image (arrows). A dilated mucosal gland can be observed in both *en face* and cross-sectional image (asterisk); F: Cross-sectional OCTA image from the solid blue lines in C and D. Subsurface capillaries in the mucosal layer can be identified as horizontal structures connecting submucosal layer to the mucosal layer (solid arrows), while the arterioles and venules can be identified as vertical structures in the submucosal layer traversing across the images (dashed arrows). Cross-sectional OCTA image was averaged over a 50 μm projection range in the longitudinal direction to improve contrast and reduce noise. Dashed and solid lines in E and F indicate 150 μm and 350 μm depth levels, respectively. Scale bars are 1 mm in A-D, 500 μm in E and F. OCT: Optical coherence tomography; OCTA: Optical coherence tomography angiography.

treated patients exhibited rectal bleeding.

Rectal OCT and OCTA features of normal and CRP patients

OCT imaging was completed in less than 10 min for each patient (mean: 8 ± 4 min, range: 4-18 min). OCT and OCTA images enabled depth-resolved visualization of rectal microstructural and microvascular architecture of patients with normal rectum (Figure 1). *En face* OCT images showed regular circular mucosal patterns characteristics of normal rectum (Figure 1A and B). Images at superficial depths showed the outline of the mucosal crypt architecture (Figure 1A) whereas images at deeper depths delineated the mucosal architecture and patterns in greater detail and contrast (owing to optical transmission and penetration from near-vertical columnar epithelium and lumens to deeper depths) (Figure 1B). *En face* OCTA images at superficial depths showed regular honeycomb-like microvascular pattern corresponding to the subsurface capillary network in the mucosal layer (Figure 1C)[25]. *En face* OCTA images at deeper depths showed rectal microvasculature corresponding to arterioles and venules in the submucosal layer, in addition to shadowing from the mucosal microvasculature (Figure 1D). The submucosal arterioles and venules had homogeneous vessel diameters of typically < 200 μm. Cross-sectional OCT images showed regular columnar architecture of normal rectum and allowed determination of mucosal and submucosal layer depths (Figure 1E)[26]. Cross-sectional OCTA images showed subsurface capillaries in the mucosal layer and arterioles and venules in the submucosal layer (Figure 1F).

OCT and OCTA images enabled depth-resolved visualization of rectal microstructural and microvascular architecture of CRP patients (Figures 2 and 3). OCT, OCTA and endoscopy images over the dentate line of an RFA-naïve CRP patient were shown in Figure 2. *En face* OCT images showed regular circular mucosal patterns on the rectal side with no apparent abnormalities (Figure 2A). *En face* OCTA images at superficial depths showed distortions on the honeycomb-like microvascular pattern, and had ectatic and tortuous microvasculature in the mucosal layer (Figure 2C). *En face* OCTA images at deeper depths showed vessels with heterogonous and unusually large diameters (> 200 μm) suggesting presence of abnormal arterioles and venules in the submucosal layer (Figure 2D). Rectal examination confirmed the OCTA

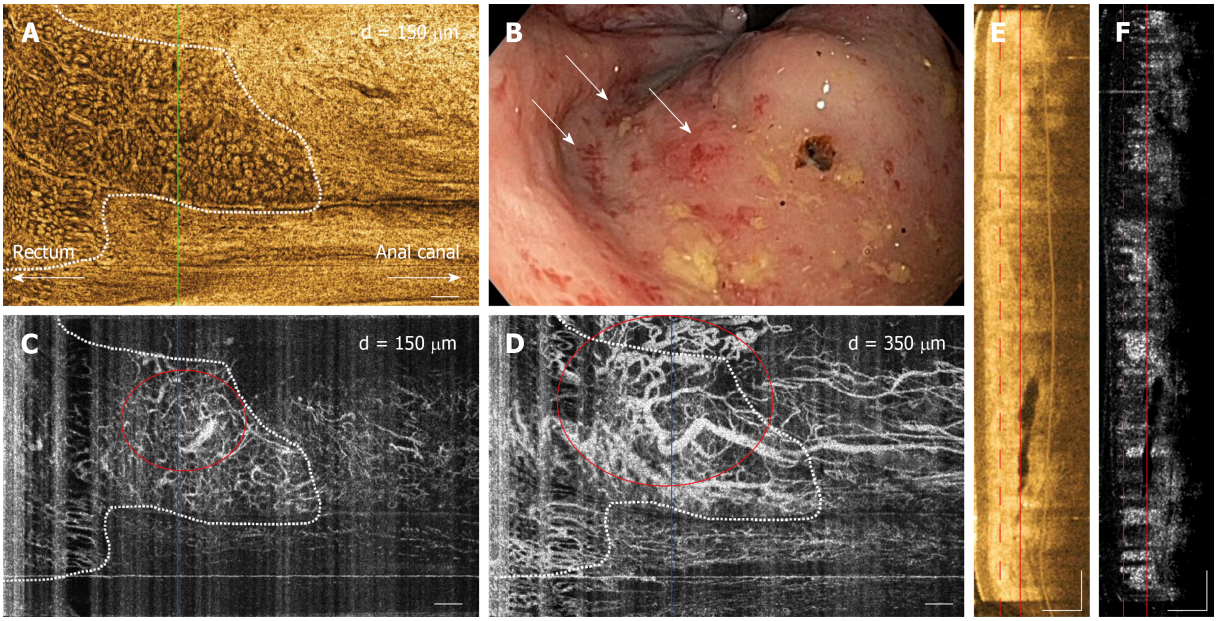

Figure 2 Depth-resolved *en face* optical coherence tomography and optical coherence tomography angiography images, cross-sectional optical coherence tomography and optical coherence tomography angiography images, and corresponding endoscopy image over the dentate line of a radiofrequency ablation-naïve chronic radiation proctopathy patient. A: *En face* optical coherence tomography (OCT) image at 150 μm depth showing regular circular mucosal patterns on the rectal side and squamous epithelium with a smooth appearance on the anal canal side; B: Shows the corresponding endoscopy image at the dentate line showing ulcerations, and edematous and non-confluent telangiectasias (rectal telangiectasia density = 2). White arrows highlight areas of telangiectasias on the rectal side; C: *En face* OCT angiography (OCTA) image at 150 μm depth showing distortions to the honeycomb-like microvascular pattern, and ectatic and tortuous rectal microvasculature (red oval) in the mucosal layer; D: *En face* OCTA image at 350 μm depth showing vessels with heterogonous and unusually large diameters (red oval) suggesting presence of abnormal arterioles and venules in the submucosal layer; E: Cross-sectional OCT image from the solid green line in A showing mucosal and submucosal layers; F: Cross-sectional OCTA image from the solid blue lines in C and D. Cross-sectional OCTA image was averaged over a 50 μm projection range in the longitudinal direction to improve contrast and reduce noise. Dashed and solid lines in E and F indicate 150 μm and 350 μm depth levels, respectively. Scale bars are 1 mm in A-D, 500 μm in E and F. OCT: Optical coherence tomography; OCTA: Optical coherence tomography angiography.

findings and the corresponding endoscopy image showed ulcerations, and edematous and non-confluent telangiectasias (Figure 2B).

OCT, OCTA and endoscopy images over the dentate line of a previously-treated CRP patient are shown in Figure 3. *En face* OCT images showed regular circular mucosal patterns on the rectal side with no apparent abnormalities (Figure 3A). *En face* OCTA images at superficial depths showed regular honeycomb-like microvascular pattern in the mucosal layer suggesting normalization of rectal mucosal microvasculature following RFA treatment (Figure 3C). *En face* OCTA images at deeper depths showed vessels with heterogonous and unusually large diameters (> 200 μm) that suggested presence of persistent abnormal arterioles and venules in the submucosal layer (Figure 3D). Corresponding endoscopy image showed healing of the rectal mucosa with some residual telangiectatic areas (Figure 3B).

Blinded OCTA reading results

Blinded OCTA reading results are given in Table 2. Occurrence of abnormal rectal OCTA features were higher in RFA-naïve patients compared with normal patients or CRP patients in RFA-follow-up visits. OCTA in 0 out of 2 (0%) normal patients, 3 out of 5 (60%) RFA-naïve patients and 0 out of 8 (0%) RFA-follow-up visits had abnormal rectal mucosal microvasculature. One out of 2 (50%) normal patients, 5 out of 5 (100%) RFA-naïve patients and 2 out of 8 (13%) RFA-follow-up visits had abnormal rectal submucosal microvasculature.

OCTA reading results for the CRP patients were also stratified according to endoscopic RTD scores (Table 3). Occurrence of abnormal rectal OCTA features increased with increasing RTD scores, suggesting a correlation of abnormal rectal microvasculature, as observed with OCTA, with the RTD scores. OCTA in 0 out of 5 (0%) visits with RTD = 0, 0 out of 3 (0%) visits with RTD = 1, 2 out of 4 (50%) visits with RTD = 2 and 1 out of 1 (100%) visit with RTD = 3 showed abnormal mucosal microvasculature. OCTA in 1 out of 5 (20%) visits with RTD = 0, 2 out of 3 (66%) visits with RTD = 1, 3 out of 4 (75%) visits with RTD = 2 and 1 out of 1 (100%) visit with RTD = 3 showed abnormal submucosal microvasculature.

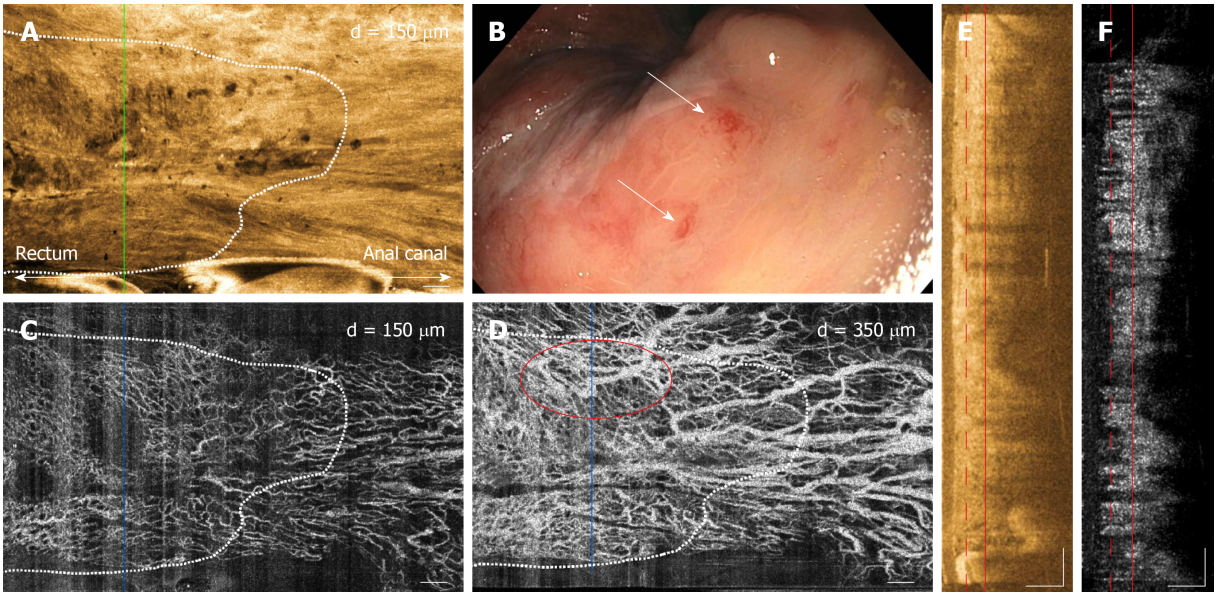

Figure 3 Depth-resolved *en face* optical coherence tomography and optical coherence tomography angiography images, cross-sectional optical coherence tomography and optical coherence tomography angiography images, and corresponding endoscopy image over the dentate line of a previously-treated chronic radiation proctopathy patient. A: *En face* optical coherence tomography (OCT) image at 150 μm depth showing regular circular mucosal patterns on the rectal side and squamous epithelium with a smooth appearance on the anal canal side; B: Shows the corresponding endoscopy image at the dentate line showing some residual telangiectatic areas (arrows, rectal telangiectasia density = 1); C: *En face* OCT angiography (OCTA) image at 150 μm depth showing regular honeycomb-like microvascular pattern in the mucosal layer; D: *En face* OCTA image at 350 μm depth showing vessels with heterogonous and unusually large diameters (red oval) suggesting presence of abnormal arterioles and venules in the submucosal layer; E: Cross-sectional OCT image from the solid green line in A showing mucosal and submucosal layers; F: Cross-sectional OCTA image from the solid blue lines in C and D. Cross-sectional OCTA image was averaged over a 50 μm projection range in the longitudinal direction to improve contrast and reduce noise. Dashed and solid lines in E and F indicate 150 μm and 350 μm depth levels, respectively. Scale bars are 1 mm in A-D, 500 μm in E and F. OCT: Optical coherence tomography; OCTA: Optical coherence tomography angiography.

DISCUSSION

Most OCT studies to date have been primarily focused on esophageal diseases, specifically on BE and its related dysplasia. Traditionally, OCT imaging speeds were limited and it was only possible to generate cross-sectional images which are complimentary to endoscopic forward-viewing (*i.e.*, *en face*) images. With advances in OCT technology, imaging speeds more than 10 times faster than current commercially-available technology are possible[24,27]. These ultrahigh speeds enable depth-resolved *en face* imaging of tissue microstructure as well as imaging microvasculature (with OCTA) which are analogous to endoscopic views and complement traditional cross-sectional OCT images. To our knowledge, this is the first study demonstrating the potential clinical utility of this next-generation OCT technology in a lower gastrointestinal tract pathology.

The depth-resolved imaging capability of OCT is a powerful advantage for assessing disease severity as well as efficacy of endoscopic treatment modalities such as RFA, where it is crucial to visualize both the treatment area and depth. A previous study on BE patients showed that presence of residual BE glands and BE epithelium thickness post-RFA predicted treatment response[28]. In addition, OCT measurements of epithelial thickness > 333 μm prior to RFA predicted the presence of residual BE on follow-up with a 92.3% sensitivity and 85% specificity. A recent study on *ex vivo* swine esophageal specimens showed that OCT can monitor RFA in real time (imaging through the ablation catheter) and quantitatively assess treatment depth using optical scattering changes of the epithelial layer during ablation[29]. Another study showed that OCT can assess the anal canal in CRP patients undergoing RFA[30], and showed re-epithelialization by neosquamous mucosa over areas of prior hemorrhage, potentially forming a protective layer preventing recurrence of bleeding. Our current study investigated depth-resolved *en face* OCT and OCTA images of the rectum from normal and CRP patients, demonstrated that rectal microvasculature in the mucosal and submucosal layers can be independently assessed and presented OCTA features of normal and abnormal rectal microvasculature. Blinded reading of the OCTA features demonstrated association of abnormal rectal microvasculature in RFA-naïve patients compared with normal patients and RFA-follow-up visits (Table 2), as well as a correlation of abnormal rectal microvasculature, as observed with OCTA, with the

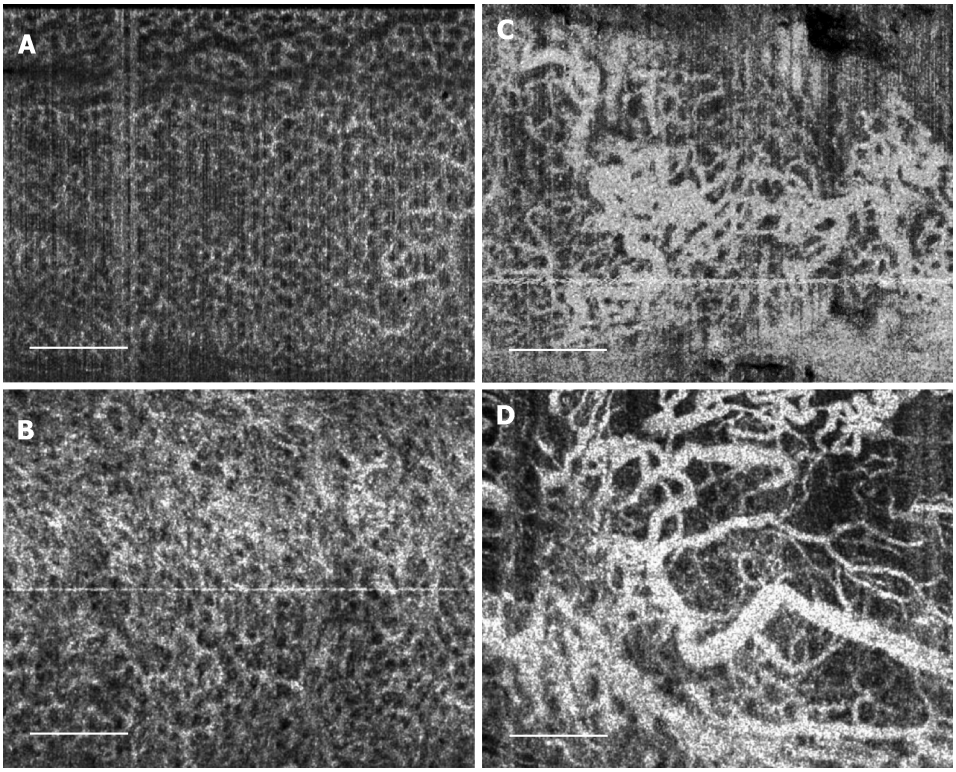

Figure 4 Summary of normal and abnormal microvasculature in the mucosal and submucosal layers of the rectum. A: Normal rectal mucosal microvasculature consisted of a honeycomb-like microvascular pattern corresponding to subsurface capillary network; B: Abnormal rectal mucosal microvasculature had distortions to the honeycomb-like microvascular pattern, and had ectatic and tortuous microvasculature; C: Normal rectal submucosal microvasculature consisted of arterioles and venules with homogeneous vessel diameters typically of < 200 μm, in addition to shadowing from the superficial mucosal microvasculature; D: Abnormal rectal submucosal microvasculature had arterioles and venules with heterogonous and unusually high vessel diameters (> 200 μm). Scale bars are 1 mm.

endoscopic RTD scores (Table 3). Altogether, these studies suggest the potential clinical utility of depth-resolved OCT and OCTA imaging in assessing disease severity of CRP as well as efficacy of endoscopic treatment modalities such as RFA.

While it is generally acknowledged that CRP is associated with angiogenic changes and corresponding tissue remodeling, the pathophysiology of CRP with regards to its onset and progression is not well elucidated[31]. A widely recognized model hypothesizes that CRP originates within the mucosal layer, where the hypoxemia caused by irradiation damages endothelial cells, inducing transcription factors such as hypoxia-inducible factor that promote angiogenic factors such as VEGF, angiogenin and FGF1[32,33]. This leads to neovascularization and dilatation of small vessels, and telangiectasia formation in the mucosal layer. According to this model, inhibition of angiogenic factors such as angiogenin and FGF1 may be a valid approach to treat CRP[33].

A recent study, on the other hand, suggested a strong role of submucosal microvascular changes leading to onset and progression of CRP[34]. Researchers collected fresh surgical rectal specimens from 30 patients with CRP and 29 patients without CRP that allowed assessment of the entire rectal wall for immunohistochemistry arrays of angiogenic factors. This was in contrast to most prior studies which evaluated rectal biopsy samples that only sampled the mucosal layer. This study found that angiostatin deposits that reside within rectal vessels are perfused throughout the mucosal-submucosal layer upon radiation damage of the endothelial cells. Angiostatins subsequently suppress microvessel formation, causing vessel stenosis and fibrotic vascular sclerosis, decreasing microvessel density in the submucosal layer[34]. The vascular changes and formation of telangiectasias in the mucosal layer are hypothesized to be compensatory changes in response to the alteration of microvasculature in the submucosal layer. This study then suggested that restoration of vascular functionality by promoting angiogenesis in the submucosal layer may help in reversing the effects of CRP.

OCTA can independently assess rectal microvasculature in the mucosa and submucosa and is well suited for studying the pathophysiology of CRP in order to develop more effective prevention and treatment approaches. OCTA allows longitudinal study of rectal microvasculature *in situ* without injected dyes or disrupting tissue integrity, unlike taking excisional biopsies or performing surgical

Table 1 Patient demographics and baseline clinical status

Patient demographics (n = 10)			
Age, mean (range)		73 (67-85)	
Sex, male, No. (%)		10 (100)	
Race, white, No. (%)		10 (100)	
CRP Patients (n = 8)			
Prior treatment	RFA-naïve, n = 5	Previously-treated, n = 3	
Prior RFA sessions, mean (range)	0 (0)	2 (1-3)	P value
Baseline RTD score, mean ± SD	2 ± 0.7	0.3 ± 0.6	0.007
Baseline Hgb, g/dL, mean ± SD	13.7 ± 1.8	12 ± 0.8	0.23

Hgb: Hemoglobin concentration; SD: Standard deviation; CRP: Chronic radiation proctopathy; RFA: Radiofrequency ablation; RTD: Rectal telangiectasia density.

resection. The results of this study demonstrated that only 3 out of 5 (60%) RFA-naïve patients had abnormal rectal mucosal microvasculature on OCTA, but all 5 out of 5 (100%) had abnormal rectal submucosal microvasculature. This may support the aforementioned recent hypothesis that CRP originates in the submucosal layer and subsequently progress to the mucosal layer[34]. Furthermore, after RFA treatment, patients had abnormal rectal mucosal microvasculature on OCTA in 0 out of 8 (0%) RFA-follow-up visits and abnormal rectal submucosal microvasculature in only 2 out of 8 (13%) RFA-follow-up visits. This may indicate that in a subset of patients RFA may not be effective for coagulating the abnormal vessels in the submucosal layer. Treatment approaches such as CSA or APC may be more appropriate to target deeper vasculature in this cohort of patients.

The OCTA reading and endoscopic RTD scoring were performed by independent researchers who were blinded to clinical status of the patients as well as each other's respective readings. Inter-observer and intra-observer agreement of these two readings was not assessed. Previous studies have showed that RTD scoring system has good inter-observer agreement, but this has not yet been widely validated[9]. However, it should be noted that OCTA is extensively used in ophthalmology and multiple techniques have been developed for automatically quantitating vasculature and vascular alterations which can be adapted to this application[35]. These software based methods will address problems of inter-observer agreement.

This study was limited in that it was retrospective and the patient enrollment was limited to the patient demographics at the clinical center and the availability of the OCT system. A fraction of patients (3 out of 8) were not imaged when they were RFA-naïve. Furthermore, RFA-follow-up patients were at different stages of treatment, and there was not a fixed interval between RFA and follow-up. Therefore, prospective studies with larger sample sizes and standardized follow-up intervals are needed to further validate the results of this study.

Typically, an endoscope is used to introduce the OCT probe into the GI tract via accessory channels. Recently, a capsule based OCT device was demonstrated for upper GI imaging which enabled wide field of view OCT imaging without requiring an endoscope[36]. In this current study, we have also demonstrated OCT imaging without requiring an endoscope by directly placing the OCT catheter onto the dentate line and rectum. OCT imaging was rapid, taking an average of 8 min per patient.

OCTA images are generated by detecting OCT signal changes caused by moving erythrocytes. Therefore, excessive OCT catheter pressure on the bowel wall may impair vascular flow and affect the visualization of smaller microvessels[37,38]. Control of catheter pressure was difficult and repeat acquisitions were performed over the same regions while applying minimal pressure, but maintaining tissue contact. During analysis, we discarded datasets that did not visualize microvasculature over all imaging depths as well as datasets exhibiting effacement of mucosal patterns (on the rectal side) as a surrogate marker for excessive catheter pressure. This problem can be addressed by designing OCT imaging devices specifically for anal/rectal applications.

The small diameter of the OCT catheter used in this study restricted the single acquisition field of view of to 10 mm × 16 mm. Although multiple acquisitions were performed to increase the imaging coverage in the longitudinal direction, only the anterior side of the rectal wall was captured in the circumferential direction. Imaging the entire circumference of the rectum is important in order to more comprehensively assess and map vascular alterations. We have recently demonstrated a tethered OCT

Table 2 Endoscopic rectal telangiectasia density scores and occurrence of abnormal rectal mucosal and submucosal microvasculature based on *en face* optical coherence tomography angiography images

Category	Total patients/visits	Endoscopy	*En face* OCTA	
		RTD ± SD	Abnormal mucosal microvasculature, *n* (%)	Abnormal submucosal microvasculature, *n* (%)
Normal patients	2	Not assessed	0 (0)	1 (50)
RFA-naïve patients	5	2.0 ± 0.7	3 (60)	5 (100)
RFA-follow-up visit	8	0.5 ± 0.8	0 (0)	2 (13)

SD: Standard deviation; RFA: Radiofrequency ablation; RTD: Rectal telangiectasia density; OCTA: Optical coherence tomography angiography.

capsule which enabled circumferential imaging over a 40 mm × 240 mm area in the esophagus in 20 seconds[39]. We also reported OCT and OCTA using a balloon-based catheter imaging in living swine, imaging over a 50 mm × 26 mm area in 18 seconds[40]. Related devices can be developed to image the proximal portion of the lower gastrointestinal tract for CRP assessment in the future[41]. OCTA/OCT imaging can be performed with a stand-alone device independent of colonoscopy, prior to colonoscopy, or with an endoscopic attachment during colonoscopy.

In summary, this study demonstrated that OCTA/OCT can visualize depth-resolved tissue microvasculature around the dentate line and rectum, relevant to assessment and treatment of CRP. We described OCTA features of normal and abnormal rectal microvasculature in the mucosa and submucosa. Blinded reading of these OCTA features suggest that submucosal vascular abnormalities are more strongly associated with CRP than mucosal vascular abnormalities. Both mucosal and submucosal vasculature was observed to normalize after RFA treatment. However, these observations must be viewed with caution because of our small patient enrollment. Submucosal vasculature is not visible endoscopically and OCTA/OCT provides a unique modality for assessing CRP. OCTA is well suited for longitudinal studies because it does not require injected dyes and can rapidly imaging large regions of rectum to yield integrated microstructural and microvascular maps. These advantages suggest that it could be a viable tool for rapid assessment of CRP to elucidate pathophysiology as well as potentially plan treatment and assess response. Further larger scale, prospective, longitudinal studies are warranted.

Table 3 Occurrence of abnormal rectal mucosal and submucosal microvasculature in chronic radiation proctopathy patients based on *en face* optical coherence tomography angiography images, stratified by endoscopic rectal telangiectasia density score

RTD	Total visits	*En face* OCTA	
		Abnormal mucosal microvasculature, *n* (%)	Abnormal submucosal microvasculature, *n* (%)
0	5	0 (0)	1 (20)
1	3	0 (0)	2 (66)
2	4	2 (50)	3 (75)
3	1	1 (100)	1 (100)

RTD: Rectal telangiectasia density; OCTA: Optical coherence tomography angiography.

ARTICLE HIGHLIGHTS

Research background

Chronic radiation proctopathy (CRP) occurs as a result of pelvic radiation therapy and is associated with formation of abnormal vasculature that may lead to persistent rectal bleeding. While incidence is declining due to refinement of radiation delivery techniques, CRP remains one of the major complications of pelvic radiation therapy and significantly affects patient quality of life. Radiofrequency ablation (RFA) is an emerging treatment modality for eradicating abnormal vasculature associated with CRP. However, questions remain regarding CRP pathophysiology and optimal disease management.

Research motivation

This pilot study utilizes ultrahigh-speed optical coherence tomography (OCT) and OCT angiography (OCTA) to investigate microvascular features of normal versus CRP patients and how they respond under endoscopic RFA treatment.

Research objectives

We utilized OCT and OCTA for assessing subsurface depth-resolved microvasculature around the dentate line and rectum of normal patients as well as CRP patients who were RFA-naïve or under treatment. OCTA can image normal and abnormal microvasculature in the mucosal and submucosal layers of the rectum, providing information not available by endoscopy. Blinded reading of vascular features were performed to assess incidence of abnormal features in RFA treatment naïve CRP as well as response under treatment. Association with endoscopic rectal telangiectasia density scoring was also investigated.

Research methods

Two patients with normal rectum and 8 patients referred for, or undergoing endoscopic treatment with RFA for CRP were imaged with ultrahigh-speed OCTA/OCT over a total of 15 OCT/colonoscopy visits (2 normal patients, 5 RFA-naïve CRP patients, 8 RFA-follow-up visits). Imaging was performed using a prototype ultrahigh-speed OCT instrument at 600 kHz axial scan rate using a small imaging catheter. OCTA enabled depth-resolved microvasculature imaging using motion contrast from flowing blood, without requiring injected dyes.

Research results

OCTA visualized normal vasculature with regular honeycomb patterns versus abnormal distorted honeycomb patterns with ectatic and tortuous microvasculature in the rectal mucosa. Normal arterioles and venules < 200 μm in diameter versus abnormal heterogenous enlarged arterioles and venules > 200 μm in diameter were visualized in the submucosa. Abnormal mucosal vasculature occurred in 0 of 2 normal patients and 3 of 5 RFA-naïve patients, while abnormal submucosal vasculature occurred more often, in 1 of 2 normal patients and 5 of 5 RFA-naïve patients. After RFA treatment, vascular abnormalities decreased, with abnormal mucosal vasculature observed in 0 of 8 RFA-follow-up visits and abnormal submucosal vasculature observed in only and 2 of 8 RFA-follow-up visits.

Research conclusions

This study demonstrated that OCTA can visualize depth-resolved normal and abnormal microvasculature around the dentate line and rectum associated with CRP and treatment response. Submucosal vascular abnormalities seemed more strongly associated with CRP than mucosal vascular abnormalities. Both mucosal and submucosal abnormal vasculature was observed to normalize after RFA treatment. However, these observations must be viewed with caution since this was a retrospective study with a small patient enrollment. Further larger scale, prospective, longitudinal studies are warranted.

Research perspectives

The role of mucosal *vs* submucosal vascular alterations in CRP remains an open question in pathophysiology. Submucosal vasculature is not visible endoscopically and therefore

OCTA/OCT provides a unique modality for assessing CRP. Furthermore, OCTA does not require injected dyes and is well suited for longitudinal studies. It can rapidly imaging large regions of rectum to yield integrated microstructural and microvascular maps. These advantages suggest that OCTA/OCT could be a viable tool for investigation of CRP to elucidate pathophysiology as well as potentially plan treatment and assess response.

REFERENCES

1 **Tagkalidis PP**, Tjandra JJ. Chronic radiation proctitis. *ANZ J Surg* 2001; **71**: 230-237 [PMID: 11355732 DOI: 10.1046/j.1440-1622.2001.02081.x]
2 **Garg AK**, Mai WY, McGary JE, Grant WH, Butler EB, Teh BS. Radiation proctopathy in the treatment of prostate cancer. *Int J Radiat Oncol Biol Phys* 2006; **66**: 1294-1305 [PMID: 17126204 DOI: 10.1016/j.ijrobp.2006.07.1386]
3 **Grodsky MB**, Sidani SM. Radiation proctopathy. *Clin Colon Rectal Surg* 2015; **28**: 103-111 [PMID: 26034407 DOI: 10.1055/s-0035-1547337]
4 **Zelefsky MJ**, Levin EJ, Hunt M, Yamada Y, Shippy AM, Jackson A, Amols HI. Incidence of late rectal and urinary toxicities after three-dimensional conformal radiotherapy and intensity-modulated radiotherapy for localized prostate cancer. *Int J Radiat Oncol Biol Phys* 2008; **70**: 1124-1129 [PMID: 18313526 DOI: 10.1016/j.ijrobp.2007.11.044]
5 **Staffurth J**; Radiotherapy Development Board. A review of the clinical evidence for intensity-modulated radiotherapy. *Clin Oncol (R Coll Radiol)* 2010; **22**: 643-657 [PMID: 20673708 DOI: 10.1016/j.clon.2010.06.013]
6 **Bazan JG**, Hara W, Hsu A, Kunz PA, Ford J, Fisher GA, Welton ML, Shelton A, Kapp DS, Koong AC, Goodman KA, Chang DT. Intensity-modulated radiation therapy versus conventional radiation therapy for squamous cell carcinoma of the anal canal. *Cancer* 2011; **117**: 3342-3351 [PMID: 21287530 DOI: 10.1002/cncr.25901]
7 **Leiper K**, Morris AI. Treatment of radiation proctitis. *Clin Oncol (R Coll Radiol)* 2007; **19**: 724-729 [PMID: 17728120 DOI: 10.1016/j.clon.2007.07.008]
8 **O'Brien PC**, Hamilton CS, Denham JW, Gourlay R, Franklin CI. Spontaneous improvement in late rectal mucosal changes after radiotherapy for prostate cancer. *Int J Radiat Oncol Biol Phys* 2004; **58**: 75-80 [PMID: 14697423 DOI: 10.1016/S0360-3016(03)01445-7]
9 **Chi KD**, Ehrenpreis ED, Jani AB. Accuracy and reliability of the endoscopic classification of chronic radiation-induced proctopathy using a novel grading method. *J Clin Gastroenterol* 2005; **39**: 42-46 [PMID: 15599209 DOI: 10.1067/mge.2003.107]
10 **Theodorescu D**, Gillenwater JY, Koutrouvelis PG. Prostatourethral-rectal fistula after prostate brachytherapy. *Cancer* 2000; **89**: 2085-2091 [PMID: 11066049 DOI: 10.1002/1097-0142(20001115)89:10<2085::AID-CNCR8>3.0.CO;2-Q]
11 **Yates MR**, Baron TH. Treatment of a radiation-induced sigmoid stricture with an expandable metal stent. *Gastrointest Endosc* 1999; **50**: 422-426 [PMID: 10462671 DOI: 10.1053/ge.1999.v50.97950]
12 **Lenz L**, Tafarel J, Correia L, Bonilha D, Santos M, Rodrigues R, Gomes G, Andrade G, Martins F, Monaghan M, Nakao F, Libera E, Ferrari AP, Rohr R. Comparative study of bipolar eletrocoagulation versus argon plasma coagulation for rectal bleeding due to chronic radiation coloproctopathy. *Endoscopy* 2011; **43**: 697-701 [PMID: 21611944 DOI: 10.1055/s-0030-1256467]
13 **Weiner J**, Schwartz D, Martinez M, Safdieh J, Aytaman A, Schreiber D. Long-term results on the efficacy of argon plasma coagulation for patients with chronic radiation proctitis after conventionally fractionated, dose-escalated radiation therapy for prostate cancer. *Pract Radiat Oncol* 2017; **7**: e35-e42 [PMID: 27663931 DOI: 10.1016/j.prro.2016.07.009]
14 **Moawad FJ**, Maydonovitch CL, Horwhat JD. Efficacy of cryospray ablation for the treatment of chronic radiation proctitis in a pilot study. *Dig Endosc* 2013; **25**: 174-179 [PMID: 23362977 DOI: 10.1111/j.1443-1661.2012.01355.x]
15 **Taylor JG**, Disario JA, Bjorkman DJ. KTP laser therapy for bleeding from chronic radiation proctopathy. *Gastrointest Endosc* 2000; **52**: 353-357 [PMID: 10968849 DOI: 10.1067/mge.2000.107726]
16 **Rustagi T**, Corbett FS, Mashimo H. Treatment of chronic radiation proctopathy with radiofrequency ablation (with video). *Gastrointest Endosc* 2015; **81**: 428-436 [PMID: 24973172 DOI: 10.1016/j.gie.2014.04.038]
17 **Jao SW**, Beart RW, Gunderson LL. Surgical treatment of radiation injuries of the colon and rectum. *Am J Surg* 1986; **151**: 272-277 [PMID: 3946764 DOI: 10.1016/0002-9610(86)90086-3]
18 **Turina M**, Mulhall AM, Mahid SS, Yashar C, Galandiuk S. Frequency and surgical management of chronic complications related to pelvic radiation. *Arch Surg* 2008; **143**: 46-52; discussion 52 [PMID: 18209152 DOI: 10.1001/archsurg.2007.7]
19 **Weiner JP**, Wong AT, Schwartz D, Martinez M, Aytaman A, Schreiber D. Endoscopic and non-endoscopic approaches for the management of radiation-induced rectal bleeding. *World J Gastroenterol* 2016; **22**: 6972-6986 [PMID: 27610010 DOI: 10.3748/wjg.v22.i31.6972]
20 **Swager A**, Boerwinkel DF, de Bruin DM, Weusten BL, Faber DJ, Meijer SL, van Leeuwen TG, Curvers WL, Bergman JJ. Volumetric laser endomicroscopy in Barrett's esophagus: A feasibility study on histological correlation. *Dis Esophagus* 2016; **29**: 505-512 [PMID: 25951873 DOI: 10.1111/dote.12371]
21 **Wolfsen HC**, Sharma P, Wallace MB, Leggett C, Tearney G, Wang KK. Safety and feasibility of volumetric laser endomicroscopy in patients with Barrett's esophagus (with videos). *Gastrointest Endosc* 2015; **82**: 631-640 [PMID: 25956472 DOI: 10.1016/j.gie.2015.03.1968]
22 **Evans JA**, Poneros JM, Bouma BE, Bressner J, Halpern EF, Shishkov M, Lauwers GY, Mino-Kenudson M, Nishioka NS, Tearney GJ. Optical coherence tomography to identify intramucosal carcinoma and high-grade dysplasia in Barrett's esophagus. *Clin Gastroenterol Hepatol* 2006; **4**: 38-43 [PMID: 16431303 DOI: 10.1016/S1542-3565(05)00746-9]
23 **Leggett CL**, Gorospe EC, Chan DK, Muppa P, Owens V, Smyrk TC, Anderson M, Lutzke LS, Tearney G, Wang KK. Comparative diagnostic performance of volumetric laser endomicroscopy and confocal laser endomicroscopy in the detection of dysplasia associated with Barrett's esophagus. *Gastrointest Endosc* 2016; **83**: 880-888.e2 [PMID: 26344884 DOI: 10.1016/j.gie.2015.08.050]
24 **Tsai TH**, Ahsen OO, Lee HC, Liang K, Figueiredo M, Tao YK, Giacomelli MG, Potsaid BM, Jayaraman V, Huang Q, Cable AE, Fujimoto JG, Mashimo H. Endoscopic optical coherence angiography enables 3-

dimensional visualization of subsurface microvasculature. *Gastroenterology* 2014; **147**: 1219-1221 [PMID: 25172015 DOI: 10.1053/j.gastro.2014.08.034]

25 **Araki K**, Furuya Y, Kobayashi M, Matsuura K, Ogata T, Isozaki H. Comparison of mucosal microvasculature between the proximal and distal human colon. *J Electron Microsc (Tokyo)* 1996; **45**: 202-206 [PMID: 8765715 DOI: 10.1093/oxfordjournals.jmicro.a023433]

26 **Adler DC**, Zhou C, Tsai TH, Schmitt J, Huang Q, Mashimo H, Fujimoto JG. Three-dimensional endomicroscopy of the human colon using optical coherence tomography. *Opt Express* 2009; **17**: 784-796 [PMID: 19158891 DOI: 10.1364/OE.17.000784]

27 **Tsai TH**, Lee HC, Ahsen OO, Liang K, Giacomelli MG, Potsaid BM, Tao YK, Jayaraman V, Figueiredo M, Huang Q, Cable AE, Fujimoto J, Mashimo H. Ultrahigh speed endoscopic optical coherence tomography for gastroenterology. *Biomed Opt Express* 2014; **5**: 4387-4404 [PMID: 25574446 DOI: 10.1364/BOE.5.004387]

28 **Tsai TH**, Zhou C, Tao YK, Lee HC, Ahsen OO, Figueiredo M, Kirtane T, Adler DC, Schmitt JM, Huang Q, Fujimoto JG, Mashimo H. Structural markers observed with endoscopic 3-dimensional optical coherence tomography correlating with Barrett's esophagus radiofrequency ablation treatment response (with videos). *Gastrointest Endosc* 2012; **76**: 1104-1112 [PMID: 22831857 DOI: 10.1016/j.gie.2012.05.024]

29 **Lee HC**, Ahsen OO, Liu JJ, Tsai TH, Huang Q, Mashimo H, Fujimoto JG. Assessment of the radiofrequency ablation dynamics of esophageal tissue with optical coherence tomography. *J Biomed Opt* 2017; **22**: 76001 [PMID: 28687822 DOI: 10.1117/1.JBO.22.7.076001]

30 **Zhou C**, Adler DC, Becker L, Chen Y, Tsai TH, Figueiredo M, Schmitt JM, Fujimoto JG, Mashimo H. Effective treatment of chronic radiation proctitis using radiofrequency ablation. *Therap Adv Gastroenterol* 2009; **2**: 149-156 [PMID: 20593010 DOI: 10.1177/1756283X08103341]

31 **Frazzoni L**, La Marca M, Guido A, Morganti AG, Bazzoli F, Fuccio L. Pelvic radiation disease: Updates on treatment options. *World J Clin Oncol* 2015; **6**: 272-280 [PMID: 26677440 DOI: 10.5306/wjco.v6.i6.272]

32 **Liu Y**, Kudo K, Abe Y, Hu DL, Kijima H, Nakane A, Ono K. Inhibition of transforming growth factor-beta, hypoxia-inducible factor-1alpha and vascular endothelial growth factor reduced late rectal injury induced by irradiation. *J Radiat Res* 2009; **50**: 233-239 [PMID: 19346676 DOI: 10.1269/jrr.08112]

33 **Takeuchi H**, Kimura T, Okamoto K, Aoyagi E, Miyamoto H, Kaji M, Takenaka H, Okamura S, Sato Y, Kato J, Okahisa T, Takayama T. A mechanism for abnormal angiogenesis in human radiation proctitis: Analysis of expression profile for angiogenic factors. *J Gastroenterol* 2012; **47**: 56-64 [PMID: 22081051 DOI: 10.1007/s00535-011-0470-2]

34 **Wu P**, Li L, Wang H, Ma T, Wu H, Fan X, Yang Z, Chen D, Wang L. Role of Angiogenesis in Chronic Radiation Proctitis: New Evidence Favoring Inhibition of Angiogenesis Ex Vivo. *Dig Dis Sci* 2018; **63**: 113-125 [PMID: 29080145 DOI: 10.1007/s10620-017-4818-1]

35 **Spaide RF**, Fujimoto JG, Waheed NK, Sadda SR, Staurenghi G. Optical coherence tomography angiography. *Prog Retin Eye Res* 2018; **64**: 1-55 [PMID: 29229445 DOI: 10.1016/j.preteyeres.2017.11.003]

36 **Gora MJ**, Sauk JS, Carruth RW, Gallagher KA, Suter MJ, Nishioka NS, Kava LE, Rosenberg M, Bouma BE, Tearney GJ. Tethered capsule endomicroscopy enables less invasive imaging of gastrointestinal tract microstructure. *Nat Med* 2013; **19**: 238-240 [PMID: 23314056 DOI: 10.1038/nm.3052]

37 **Holloway GA**, Daly CH, Kennedy D, Chimoskey J. Effects of external pressure loading on human skin blood flow measured by 133Xe clearance. *J Appl Physiol* 1976; **40**: 597-600 [PMID: 931880 DOI: 10.1152/jappl.1976.40.4.597]

38 **Choi WJ**, Wang H, Wang RK. Optical coherence tomography microangiography for monitoring the response of vascular perfusion to external pressure on human skin tissue. *J Biomed Opt* 2014; **19**: 056003 [PMID: 24810259 DOI: 10.1117/1.JBO.19.5.056003]

39 **Liang K**, Ahsen OO, Lee HC, Wang Z, Potsaid BM, Figueiredo M, Jayaraman V, Cable AE, Huang Q, Mashimo H, Fujimoto JG. Volumetric Mapping of Barrett's Esophagus and Dysplasia With en face Optical Coherence Tomography Tethered Capsule. *Am J Gastroenterol* 2016; **111**: 1664-1666 [PMID: 27808130 DOI: 10.1038/ajg.2016.419]

40 **Lee HC**, Ahsen OO, Liang K, Wang Z, Cleveland C, Booth L, Potsaid B, Jayaraman V, Cable AE, Mashimo H, Langer R, Traverso G, Fujimoto JG. Circumferential optical coherence tomography angiography imaging of the swine esophagus using a micromotor balloon catheter. *Biomed Opt Express* 2016; **7**: 2927-2942 [PMID: 27570688 DOI: 10.1364/BOE.7.002927]

41 **Trindade AJ**, Sultan K, Vamadevan AS, Fan C, Sejpal DV. Successful use of volumetric laser endomicroscopy in imaging a rectal polyp. *Therap Adv Gastroenterol* 2016; **9**: 128-131 [PMID: 26770274 DOI: 10.1177/1756283X15615309]

Published By Baishideng Publishing Group Inc
7041 Koll Center Parkway, Suite 160, Pleasanton, CA 94566, USA
Telephone: +1-925-2238242
Fax: +1-925-2238243
E-mail: bpgoffice@wjgnet.com
Help Desk:http://www.f6publishing.com/helpdesk
http://www.wjgnet.com